BIOCHEMISTRY
including biophysical chemistry & molecular biology

Article

pubs.acs.org/biochemistry

A Novel Role for Coenzyme A during Hydride Transfer in 3-Hydroxy-3-methylglutaryl-coenzyme A Reductase

C. Nicklaus Steussy,[†] Chandra J. Critchelow,[†] Tim Schmidt,[†] Jung-Ki Min,[‡] Louise V. Wrensford,[§] John W. Burgner, II,[†] Victor W. Rodwell,[∥] and Cynthia V. Stauffacher*[,⊥]

[†]Department of Biological Sciences, Purdue University, West Lafayette, Indiana 47907, United States

[‡]Department of Biochemistry, Duke University School of Medicine, Durham, North Carolina 27710, United States

[§]Department of Chemistry, Albany State University, Albany, Georgia 31705, United States

[∥]Department of Biochemistry, Purdue University, West Lafayette, Indiana 47907, United States

[⊥]Department of Biological Sciences and Purdue Center for Cancer Research, Purdue University, West Lafayette, Indiana 47907, United States

ABSTRACT: In this study, we take advantage of the ability of HMG-CoA reductase (HMGR) from *Pseudomonas mevalonii* to remain active while in its crystallized form to study the changing interactions between the ligands and protein as the first reaction intermediate is created. HMG-CoA reductase catalyzes one of the few double oxidation−reduction reactions in intermediary metabolism that take place in a single active site. Our laboratory has undertaken an exploration of this reaction space using structures of HMG-CoA reductase complexed with various substrate, nucleotide, product, and inhibitor combinations. With a focus in this publication on the first hydride transfer, our structures follow this reduction reaction as the enzyme converts the HMG-CoA thioester from a flat sp^2-like geometry to a pyramidal thiohemiacetal configuration consistent with a transition to an sp^3 orbital. This change in the geometry propagates through the coenzyme A (CoA) ligand whose first amide bond is rotated 180° where it anchors a web of hydrogen bonds that weave together the nucleotide, the reaction intermediate, the enzyme, and the catalytic residues. This creates a stable intermediate structure prepared for nucleotide exchange and the second reduction reaction within the HMG-CoA reductase active site. Identification of this reaction intermediate provides a template for the development of an inhibitor that would act as an antibiotic effective against the HMG-CoA reductase of methicillin-resistant *Staphylococcus aureus*.

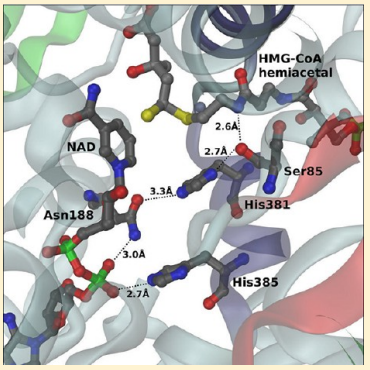

Over the last hundred years, our understanding of how enzymes facilitate chemical reactions in cells has improved by orders of magnitude. However, even as we study the enzymes, substrates, products, and cofactors, often the dynamic process of catalysis eludes us for want of being able to visualize the intermediate states of the reaction. In this study of HMG-CoA reductase (HMGR) from *Pseudomonas mevalonii*, we take advantage of the fact that the enzyme is active in the crystalline form, catalyzing the double-reduction reaction of HMG-CoA to mevalonate and free coenzyme A (CoA) utilizing two molecules of nicotinamide adenine dinucleotide (NADH). We have used X-ray crystallography to study more than 70 structures covering this reaction space of the enzyme with various combinations of ligands, substrates, and inhibitors. What has emerged is a novel contribution by CoA to the catalytic process driven by the change in geometry around the HMG-CoA thioester during the first hydride transfer.

The reaction catalyzed by HMG-CoA reductase is the first committed step in the metabolic pathway that produces the five-carbon compound isopentenyl diphosphate. This metabolite is the building block for cholesterol, ubiquinone, the carbohydrate anchor dolichol, prenyl groups, and steroid-based hormones in animals,[1] light-harvesting carotenoids in plants,[2] and cell-wall undecaprenol in eubacteria.[3]

The eukaryotic and prokaryotic isoforms of HMG-CoA reductase are different and can be distinguished both by amino acid sequence alignments and by their sensitivity to statin inhibitors.[4] X-ray crystal structures of the enzymes have shown their catalytic domains have the same overall fold but distinct active site architectures.[5] Of note is the fact that a number of bacteria that utilize the mevalonate pathway are potent pathogens, such as *Staphylococcus aureus*, *Streptococcus pneumoniae*, and *Enterococcus faecalis*, and the pathway has been shown to be essential to their growth and pathogenesis.[6] This observation gives rise to an interest in developing a small molecule inhibitor specific to the bacterial HMG-CoA reductases. Such an inhibitor would act as a novel antibiotic, effective against the increasing number of resistant bacterial strains, such as methicillin-resistant *S. aureus* (MRSA) and

Received: March 14, 2013
Revised: May 28, 2013
Published: June 26, 2013

   dx.doi.org/10.1021/bi400335g | *Biochemistry* 2013, 52, 5195−5205

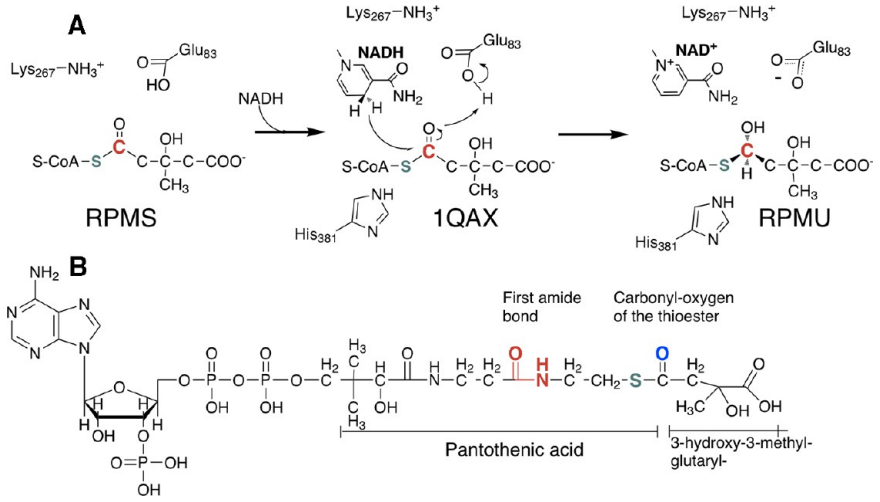

Figure 1. Chemistry of hydride transfer and the structure of HMG-CoA. (A) Schematic of the first hydride transfer of HMG-CoA reductase. On the left is HMG-CoA schematically arranged with some of the residue side chains known to be important in catalysis. Here the thioester is in a flat, sp^2 orbital configuration with the carbonyl carbon colored red. This cartoon represents the RPMS structure. NADH is then bound and the hydride transferred from the C4 position of the nicotinamide ring to the sp^2 carbon. The previously published structure of the nonproductive complex of NAD and HMG-CoA (Protein Data Bank entry 1QAX) serves as the best representative of this dynamic state. The hydride transfer then converts the thioester to the hemiacetal with a tetrahedral sp^3 orbital configuration (RPMU). Lys267 has been suggested as the proton donor for the reaction based on the earlier 1QAX structure.[9] Our hemiacetal structure suggests that Glu83 is a more likely candidate, and this has been supported with computational experiments.[32] The mechanism of the first hydride transfer of the reaction mechanism only is illustrated; the entire mechanism is outlined in ref 32. (B) 3-Hydroxy-3-methylglutaryl-coenzyme A (HMG-CoA). Structure of the ligand for HMG-CoA reductase with emphasis on the portions discussed in the text. The first amide bond that forms the basis of the hydrogen bonding network with hemiacetal formation is colored red. Sulfur is substituted for the carbonyl oxygen of the thioester bond in the dithio-HMG-CoA slow substrate used to trap the hemiacetal intermediate (in blue). This figure was prepared using ChemDraw.[33]

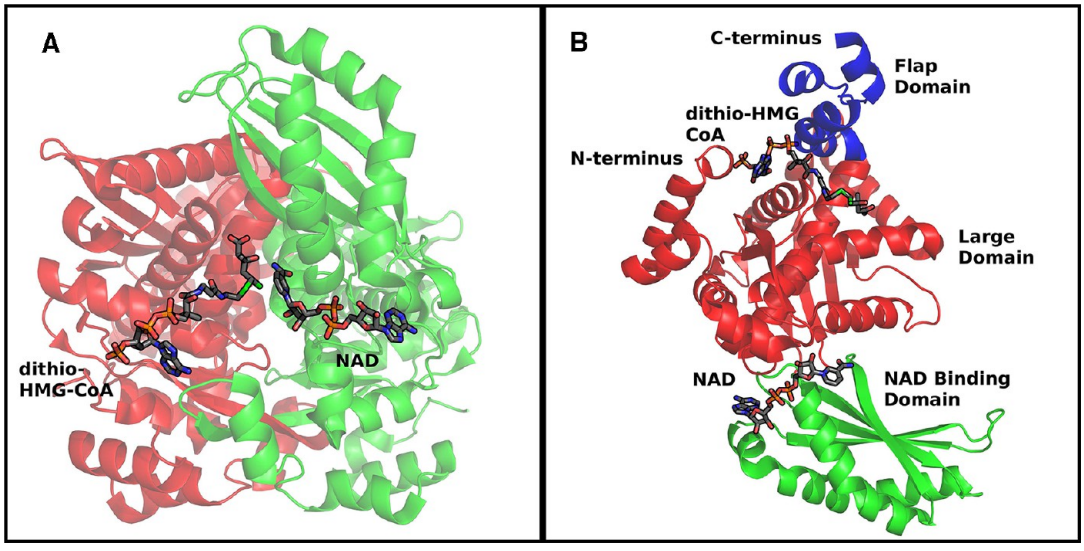

Figure 2. Domain structure of HMGR from *P. mevalonii*. (A) A dimer of HMGR (structure RPMU) with the bound substrate and cofactor. The two monomers intertwine with the active site at their interface. The 53 residues of the C-terminal flap domain have been removed to expose the configuration of the ligands in the active site. (B) One monomer, rotated around a complex axis to best demonstrate the domain structure, bringing the green NAD binding domain to the bottom of the figure and the central helix of the triangular large domain to a 45° position in the plane of the figure. In this panel, the large domain (red) is composed of residues 1−108 and 220−349 and binds the dithio-HMG-CoA. The NAD binding domain (green) contains residues 109−219 and binds the NAD(H) for the opposite active site. The C-terminal flap domain (blue) contains three helices of residues 375−421 and is seen only when both ligands are bound. This figure was prepared using Pymol.[34]

vancomycin-resistant *Enterococcus* (VRE), which are widespread in today's intensive care units.

The overall reaction sequence and stoichiometry of the double reduction of HMG-CoA to mevalonate and free CoA have been worked out over the past few decades. Figure 1A shows a schematic diagram for the first hydride transfer in the synthesis of mevalonate, in which HMG-CoA is first bound to the enzyme along with 1 equiv of NADH. There is no evidence in the literature that this binding occurs in any particular sequence, though in our crystallographic studies the cofactor NAD(H) is never seen unless another ligand is present. The transfer of a hydride from NADH reduces the thioester bond between CoA and 3-hydroxy-3-methylglutarate, resulting in a sequestered reaction intermediate thought to be a thiohemia-

dx.doi.org/10.1021/bi400335g | *Biochemistry* 2013, 52, 5195−5205

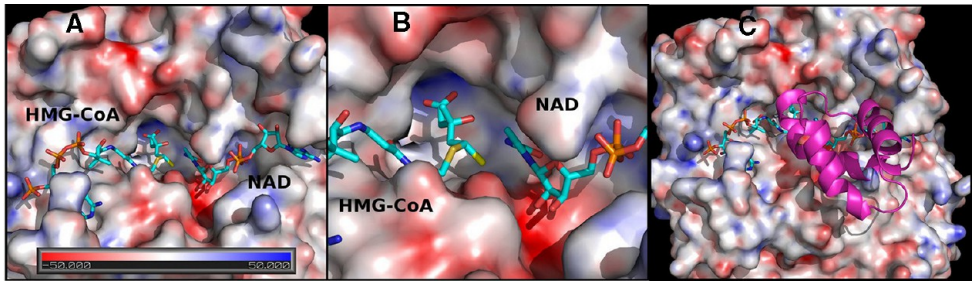

Figure 3. Electrostatic surface of HMGR with HMG-CoA and NAD(H). (A) HMG-CoA (data set RPMU) is shown binding to the enzyme in a shallow groove along the surface. The adenine of the CoA, on the left of the figure, is obscured by the side chain of Arg11 that covers the nucleotide. The dithioester between CoA and HMG is shown here in the hemiacetal configuration, with the sulfurs (yellow) toward the middle of the figure. NAD(H) is bound in a surface groove to the right. Its adenine is partially obscured by the side chains of the conserved DAMG sequence associated with the non-Rossmann nucleotide-binding domain of the enzyme. The nicotinamide ring of NAD(H) and the thioester bond of HMG-CoA come into catalytic contact in the center of the figure, shown in more detail in panel B. (C) Flap domain in a ribbon cartoon form, positioned over the active site by the hydrogen bonding interactions associated with hemiacetal formation. This figure was prepared using Pymol.[34]

cetal. This thiohemiacetal would then be in equilibrium with the reduced CoA and mevaldehyde, the aldehyde thought to be the active substrate for the second reduction reaction.[7] The NAD^+ is released to solution in preparation for binding of another NADH for the second hydride transfer that converts the aldehyde to an alcohol, mevalonate.

Published X-ray crystal structures of the *P. mevalonii* HMGR show that the molecule is a tightly bound, intertwined dimer with each monomer consisting of a large domain, a small domain, and a C-terminal flap region (Figure 2).[8,9] The large domain is discontinuous, constructed from the first 100 amino acids and then residues 220−375, and is primarily involved in binding the CoA portion of HMG-CoA. Between the two components of the large domain is a region termed the "small domain" that folds into a non-Rossmann nucleotide binding domain[10] whose residues interact with the adenine and phosphates of the NAD(H). Finally, the 50 C-terminal residues of the "flap" domain are disordered in the apoenzyme. The flap has been observed only in an experiment in which the ligands NAD^+ and HMG-CoA were soaked into a preformed crystal to form a complex with no reaction potential [Protein Data Bank (PDB) entry 1QAX]. In this experiment, these residues form a subdomain consisting of three α-helices folded over the active site, positioning catalytic residue His381 near the site of hydride transfer and shielding this reduction reaction from solvent (Figure 3c).[9]

Gaps in our understanding of the catalytic reaction of HMG-CoA reductase remain. Previous investigations have been unable to isolate a structure with HMG-CoA alone bound to the enzyme as the thioester bond appears to degrade during X-ray data collection (PDB entry 1R31), leaving free CoA and mevalonate or mevaldehyde in the active site. In addition, the intermediate configuration of HMG-CoA after hydride transfer and its interaction with catalytic residues in the active site are unknowns. Finally, the observation that the addition of CoA, even desthio-CoA, markedly increases the V_{max} of the mevaldehyde to mevalonate half-reaction remains unexplained.[11] The investigations presented here were undertaken to answer these questions; what was discovered was a set of successive ligand−protein interactions that drive the reaction to a stable intermediate state.

EXPERIMENTAL PROCEDURES

HMG-CoA reductase from *P. mevalonii* has been cloned into the PKK-177-3 plasmid under control of the *tac* promoter and kanamycin selection.[12] Expression, purification, and crystallization have been described previously.[13] Briefly, the protein was dialyzed into a solution containing 10 mM potassium phosphate, 400 mM potassium chloride, and 9% (v/v) glycerol at pH 7.2. It was then concentrated to 20 mg/mL. Crystallization was accomplished by vapor phase exchange against a reservoir solution containing 1.3−1.4 M ammonium sulfate and 100 mM sodium ADA at pH 6.7. The protein solution was seeded with 0.8 μL of crushed reductase crystals serially diluted 10^3−10^4-fold with the precipitant solution. Of particular importance is the use of glycerol during purification and crystallization to produce large, diffraction quality crystals. The concentration of glycerol is increased again to 30% as a cryoprotectant before data collection.

Introduction of ligands into preformed crystals of reductase was accomplished by a slow replacement of the mother liquor in a sitting drop with gradually increasing amounts of glycerol (for cryoprotection) and ligand(s). Extending this procedure over many hours yielded crystals that were cryoprotected and consistently diffracted to better than 2.0 Å at a synchrotron beamline. The data sets are designated RPM for reductase *P. mevalonii*, with an alphanumeric suffix to mark the particular experiment.

RPM2QS (PDB entry 4I64). This is a native crystal cryoprotected with 30% glycerol as described above.

RPM3SS (PDB entry 4I6A). The crystal was cryoprotected in 30% PEG400, rather than glycerol, that was gradually introduced over 17.5 h. Then HMG-CoA was introduced into the cryosolution at a concentration of 4 mM for 4.5 h prior to the crystals being frozen.

RPMS (PDB entry 4I56). Glycerol was gradually introduced to the crystal soaking solution over 12 h. Dithio-HMG-CoA (the carbonyl oxygen of the thioester bond is replaced by a sulfur atom; preparation discussed below) was added to a final concentration of 3.15 mM over 4 h.

RPMU (PDB entry 4I4B). After the crystals had been soaked in 30% glycerol for 12 h, 3.3 mM dithio-HMG-CoA and 1.5 mM NADH were added sequentially to the solution and allowed to react for 9 h prior to the crystals being frozen.

Once the crystals were soaked with an appropriate cryosolution and a ligand, they were frozen in a stream of 100 °K gaseous nitrogen. An initial data set was collected on our home source, a Rigaku RU-200 rotating anode generator equipped with confocal mirrors and a RaxisIV^{++} detector, to confirm diffraction. A maximal resolution data set would then

dx.doi.org/10.1021/bi400335g | *Biochemistry* 2013, 52, 5195−5205

Table 1. Data Collection and Refinement Statistics[a]

	RPM2QS	RPM3SS	RPMS	RPMU
		Data Collection		
PDB entry	4I64	4I6A	4I56	4I4B
ligands added	native (none)	HMG-CoA	dithio-HMG-CoA	dithio-HMG-CoA NADH[b]
location	APS 14-BM-C	APS 17-ID	APS 14-BM-C	APS 14-BM-C
energy (Å)	0.9	1.0	0.9	0.9
space group	*I*4(1)32	*I*4(1)32	*I*4(1)32	*I*4(1)32
$a = b = c$ (Å)	225.6	225.7	226.1	225.9
resolution (Å)	25−1.75	39−1.85	29−1.50	29−1.70
no. of observations $>1\sigma$	821771	2841960	803028	398341
no. of rejections (%)	2224 (0.3)	3314 (0.2)	868 (0.1)	695 (0.2)
no. of unique reflections	95865	82730	150297	102738
no. of R_{free} reflections	2931	2479	10622	7396
completeness (%)	98.4 (100)	99.9 (100)	97.6 (88.9)	96.4 (93.2)
redundancy	8.6 (7.1)	34.0 (33.0)	5.4 (2.4)	3.9 (2.6)
$I/\sigma I$	26.8 (2.1)	48.1 (3.3)	27.3 (2.4)	25.9 (1.8)
R_{merge} (%)	5.7 (89.6)	7.1 (0.871)	4.3 (33.1)	4.7 (40.3)
		Refinement		
total no. of atoms	6318	6146	6477	6747
no. of protein atoms (avg *B*)	5679 (32.0)	5661 (35.9)	5628 (20.1)	5855 (28.6)
no. of waters (avg *B*)	609 (43.4)	420 (43.3)	761 (33.0)	757 (40.8)
no. of ligand/ion atoms (avg *B*)	30 (62.6)	63 (49.8)	86 (32.3)	135 (31.7)
R_{work}/R_{free}	0.198/0.246	0.178/0.200	0.168/0.189	0.173/0.195
rmsd for bonds (Å)	0.005	0.022	0.020	0.005
rmsd for angles (deg)	0.92	1.45	1.74	1.13
Molprobity score (%)	95	99	94	100
Ramachandran				
preferred	639 (98.9)	642 (99.1)	640 (99.1)	673 (99.1)
generous	5 (0.8)	4 (0.6)	4 (0.6)	4 (0.6)
disallowed[c]	2 (0.3)	2 (0.3)	2 (0.3)	2 (0.3)

[a]Data from the last (highest) resolution bin are given in parentheses. [b]NADH was added to the crystal; structural evidence suggests it was oxidized to NAD^+. [c]The residues in the disallowed region for all structures are Arg182 and Arg682, identical residues in the A and B monomers, respectively.

be taken at one of several beamlines at the Advanced Photon Source (Argonne National Laboratory, Argonne, IL) (see Table 1).

The early diffraction data were reduced with DENZO and SCALEPACK and later data sets with HKL2000.[14] Phasing was accomplished by molecular replacement with CNS using the high-resolution native structure of HMG-CoA reductase (RPM2QS) as a search model.[15] Subsequent building of ligand models into the nonprotein density used the HIC-UP server[16] to provide a starting set of coordinates.

The geometry and energy parameters of the ligand models were corrected on the basis of the atomic resolution, small molecule structures available through the Cambridge Small Molecule Database.[17] These specialized topology and parameter files for the ligands were then used to refine the protein−solvent−ligand model using CNS. Subsequent corrections to the protein and ligand were made using the interactive graphics capability of O,[18,19] followed by conjugate-gradient (Powell) minimization in CNS. In the later stages of the project, a final refinement pass in Refmac5[20] using the TLS refinement[21] interspersed with maximum likelihood minimization[20] was added.

During refinement, a control group of reflections was kept aside to monitor progress.[22,23] These control reflections were maintained across the four structures and two refinement programs. Postrefinement, the model structures were evaluated for errors with Molprobity,[24] Procheck,[25] and the ADIT Validation server of the PDB.[26] Selected quality indicators are listed in Table 1.

The protein crystallized as a dimer in the asymmetric unit, with one active site open to a solvent channel and the other limited by crystallographic contacts. The residues of the first monomer, the one with the open HMG-CoA binding site, were numbered starting with 1, while the numbering of the second monomer starts with 500. Thus, Lys267 and Lys767 would be the same residue on the A and B polypeptide chains, respectively. When soaking in ligands, the larger molecules were invariably seen in the more open site and not in the closed one. Because of these differences between the active sites of the dimer, NCS restraints on refinement were not used.

Dithio-HMG-CoA. The substrate analogue dithio-HMG-CoA was used to demonstrate a binary, dithio-HMG-CoA−enzyme structure and to trap the hemiacetal intermediate in a ternary dithio-HMG-CoA−NADH−enzyme complex. In this compound, the carbonyl oxygen of the thioester of HMG-CoA is replaced with sulfur (Figure 1). This molecule is stereospecifically synthesized using the enzyme HMG-CoA synthase (acetyl-CoA + acetoacetyl-CoA → HMG-CoA + CoA-SH), by substituting 3-oxo-1-thiobutyryl-CoA for the usual acetoacetyl-CoA. The resulting dithio-HMG-CoA compound was initially characterized as an inhibitor of HMGR with a K_i of 86 nM and with a competitive pattern versus HMG-CoA.[22] Further study in our laboratory showed this compound to be a slow substrate, as related in Results.

dx.doi.org/10.1021/bi400335g | *Biochemistry* 2013, 52, 5195−5205

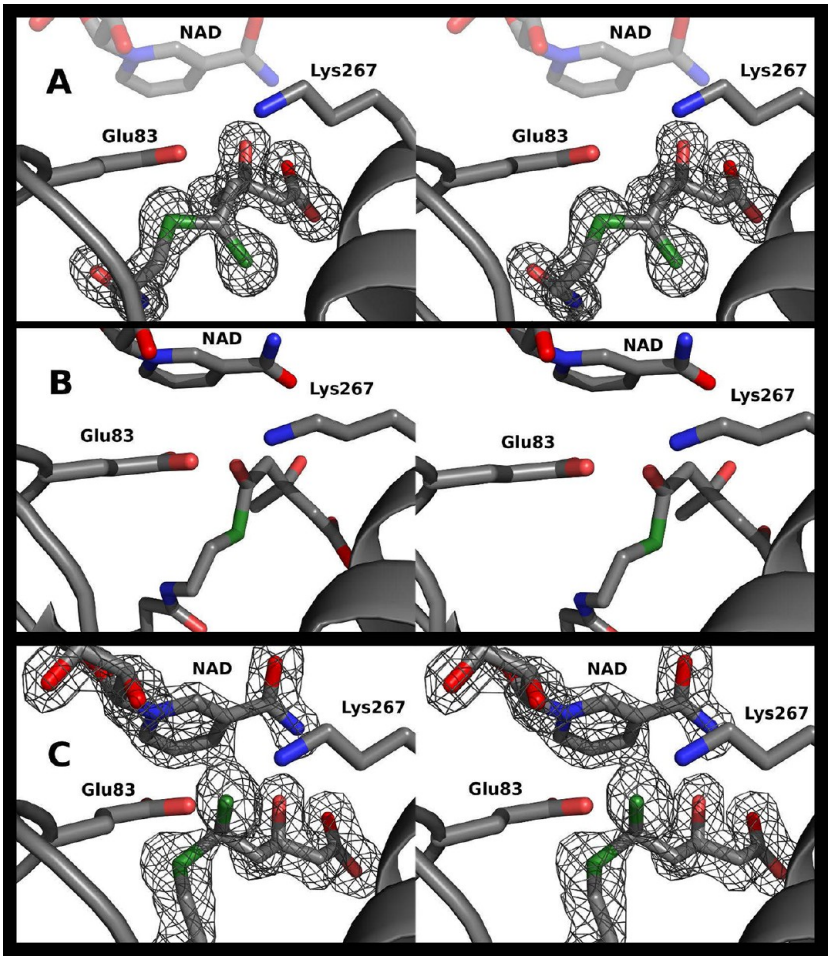

Figure 4. Evolution of the thioester bond during the first hydride transfer. (A) Initial binding (data set RPMS) of HMG-CoA to HMG-CoA reductase from *P. mevalonii*. Depicted is the structure with the slow substrate, dithio-HMG-CoA, where the carbonyl carbon is replaced by a (green) sulfur atom. The electron density shown is a simulated annealing omit $F_o - F_c$ map (CNS version 1.3[15]) contoured at 3.0σ. The NAD^+ in the panel is not actually present in the structure but is there for the purpose of orientation, shown at the location of the cofactor in RPMU. Note the flat geometry of the dithioester bond consistent with an unreduced sp^2 orbital and its orientation away from the nicotinamide ring (HMGCoA C1−NAD C4 distance of 5.1 Å). (B) Nonproductive complex containing NAD^+ and HMG-CoA (PDB entry 1QAX).[9] This models the movement of the thioester as the nucleotide binds with the thioester bond rotated up toward the NAD^+ while retaining its flat sp^2 orbital-like geometry (HMGCoA C1−NAD C4 distance of 4.0 Å). (C) Dithioester (data set RPMU) of the slow substrate reduced to the hemiacetal form, and therefore the end result of the first hydride transfer. The dithioester now has a pyramidal geometry consistent with a reduced, sp^3 orbital configuration oriented roughly parallel to the nicotinamide ring, with the former "carbonyl" atom directed upward toward active site residues Glu83 and Lys267 (HMGCoA C1−NAD C4 distance of 3.2 Å). The electron density shown is a simulated annealing omit $F_o - F_c$ map (CNS version 1.3[15]) contoured at 3.0σ. This figure was prepared using Pymol.[34]

GLIDE. The estimates of relative binding energies between HMGR and the HMG-CoA configurations (1QAX, RPMS, RPMU) were calculated using the software package GLIDE from Schrödinger (Glide, version 5.7, Schrödinger, LLC, New York, NY, 2011). The ligands and protein were kept in a rigid configuration given in the associated X-ray crystal structure and the GlideScore calculated and interpreted as a proxy for a relative binding energy (23).

S85A Mutation. Conversion of serine 85 of *P. mevalonii* HMGR to alanine used a Stratagene QuikChange Site-Directed Mutagenesis Kit and protocol. Plasmid pHMGR DNA was prepared using a Qiagen Miniprep kit. Primers were synthesized by Integrated DNA Technologies, Inc. The forward primer (5′-AAGAGCCCGCAATCGTCGCCGCT-3′) and the reverse primer (5′-AGCGGCGACGATTGCGGGCTCTT-3′) were used for mutagenesis. The mutation was verified by full-length DNA sequencing in the Purdue Genomics Core.

BL21(DE3) cells transformed with mutant plasmid were grown at 37 °C, with shaking, in LB medium. Cell rupture and enzyme purification through the DEAE fraction were conducted as previously described.[12] The DEAE fraction was concentrated by precipitation with 3 volumes of a saturated ammonium sulfate solution (pH 7.0) and dissolved in a minimal volume of buffer A [10 mM potassium phosphate, 400 mM KCl, and 9% glycerol (pH 7.2)]. After dialysis against buffer A and passage through a 0.22 μm cellulose acetate filter (Nalgene), the DEAE fraction was applied to a Hiprep 26/60 Sephacryl S 200 (GE Healthcare) column equilibrated and eluted with buffer A at a flow rate of 1.3 mL/min. Active fractions were pooled and concentrated using ammonium sulfate as described above.

Assay for Enzyme Activity. The oxidative acylation of mevalonate was used to assay the activity of mutant enzyme HMGR S85A. Assays, with a final volume of 200 μL, contained 5 mM (*R*,*S*)-mevalonate, 1 mM CoASH, 1.5 mM NAD^+, 0.1 M

dx.doi.org/10.1021/bi400335g | *Biochemistry* 2013, 52, 5195−5205

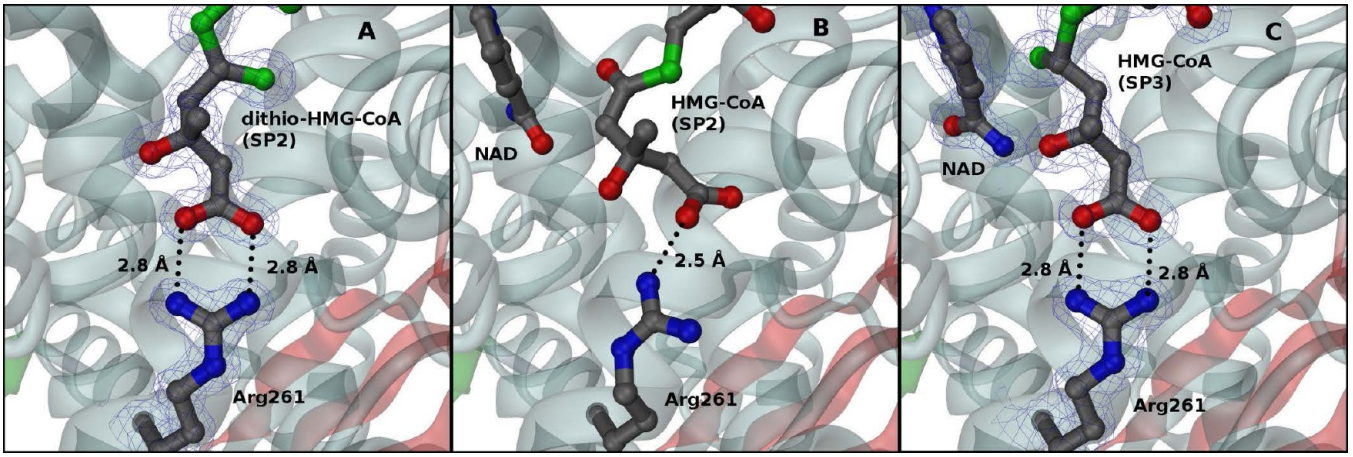

Figure 5. Hydrogen bonding between HMG-CoA and Arg261 through the reaction cycle. (A) Structure of RPMS, with only the dithio-HMG-CoA bound. The ester bond is in a flat, sp^2 orbital, and there are two hydrogen bonds between the glutaryl portion of HMG-CoA and Arg261. (B) Structure developed from the nonproductive complex of NAD^+ and HMG-CoA (PDB entry 1QAX) that serves here as a model for the intermediate in the reaction in which HMG-CoA and NADH are both bound but the hydride transfer has not yet taken place. The thioester thus remains in the flat sp^2 orbital configuration but has reoriented toward the active site residues. Adjusting to this motion, the glutaryl group changes its orientation relative to Arg261, and the side chain of the amino acid flips, such that only one hydrogen bond is formed between the two. (C) RPMU in which the thioester of dithio-HMG-CoA has been reduced to the hemiacetal. The tetrahedral configuration of the bond is evident. This conversion allows the glutaryl moiety and Arg261 to regain their original orientation, forming two hydrogen bonds. The electron density shown in panels A and C is 1.4σ, $2F_o - F_c$ density from the refined model. The red and green β-strands toward the back of the figure are from monomers A and B of the dimer, respectively.

KCl, and 0.1 M Tris (pH 9.0). Formation of NADH was monitored at 340 nm in a Hewlett-Packard model 8453 diode array spectrophotometer with its cell compartment maintained at 37 °C.[27]

RESULTS

HMG-CoA Structure. The previous structural work on prokaryotic HMGR had shown the mechanism to be dynamic, with large domain movements during catalysis.[8,9] The trigger for this motion was not known, nor was there a structure with only an intact HMG-CoA bound to the enzyme. Previous experiments in which HMG-CoA was soaked into preformed crystals revealed the thioester bond to be broken (PDB entry 1R31). This was presumed to be due to exposure to the high-intensity X-ray beam during data collection. The substrate analogue dithio-HMG-CoA was initially used to create the dithio-HMG-CoA−enzyme binary complex (RPMS) that was stable in the X-ray beam. Subsequent investigation showed that substituting PEG 400 for glycerol as a cryoprotectant allowed the collection of a binary complex with normal HMG-CoA without lysis of the thioester bond (RPM3SS).

These structures of the enzyme bound to either HMG-CoA or dithio-HMG-CoA were remarkably different than expected. The thioester bond was flat and intact, consistent with an unreduced C1 atom. However, the plane of that bond was rotated 120° away from that seen in the nonproductive NAD^+−HMG-CoA structure (PDB entry 1QAX). This positioned the carbonyl oxygen of the HMG-CoA thioester (RPM3SS) and the substituted sulfur in the ligand analogue (RPMS) more than 6.0 Å from the active site catalytic residues Glu83 and Lys267 (Figure 4A). In addition, modeling the position of the nicotinamide ring from the nonproductive complex showed the C4 atom hydride donor in the nicotinamide ring and the HMG-CoA C1 atom hydride acceptor were 5.1 Å apart. This configuration of the substrate was clearly far from the ideal geometry for hydride transfer.

The remainder of the HMG-CoA's interaction with the enzyme shows that it is tightly anchored by hydrogen bonds to the protein at both ends. Specifically, Arg11 makes a hydrophobic contact between the CoA adenine and its side chain carbons and a hydrogen bond between the imine group and the adenine phosphate (3.0 Å). At the other end, the carboxyl group of HMG has two hydrogen bonds to the imine group of Arg261 [both 2.8 Å (Figure 5A)]. Between these two anchors, the interactions are water-mediated, leading to a great deal of torsional flexibility in the middle of the HMG-CoA ligand.

Dithio-HMG-CoA Is a Slow Substrate. Dithio-HMG-CoA is an analogue of HMG-CoA in which the thioester oxygen is replaced with sulfur. Previous investigations have shown this molecule to be a competitive inhibitor of HMGR, with a K_i of 86 nM.[28] The possibility that this might be a slow substrate rather than an inhibitor was suggested by analogous studies of the reduction by NADH of thiopyruvate to thiolactate by lactate dehydrogenase.[29] To investigate this possibility, the absorption spectrum for a reaction mixture that contained 20 μM *S. aureus* HMGR (vs 18 pM for the Wrensford study), 30 μM dithio-HMG-CoA, and 80 μM NADH was measured at 4 min intervals (Figure 6A). The scan with a maximum near 312 nM (red line) is the spectrum of the HMGR−dithio-HMG-CoA binary complex prior to starting the reaction by addition of NADH. The other spectra show that NADH is partially oxidized by the dithio compound as expected on the basis of the excess NADH present.

A second study (Figure 6B) shows a plot of the absorbance at 340 nm versus time for the same reaction mixture as the first. This shows a triphasic reaction profile with an initial "burst phase" followed immediately by a zero-order (steady state) phase. These data were fit by nonlinear least squares to the equation shown in the inset of Figure 6B. The half-life of the burst phase is ~0.5 min, and the magnitude of the burst corresponds to the oxidation of one enzyme equivalent of

dx.doi.org/10.1021/bi400335g | *Biochemistry* 2013, 52, 5195−5205

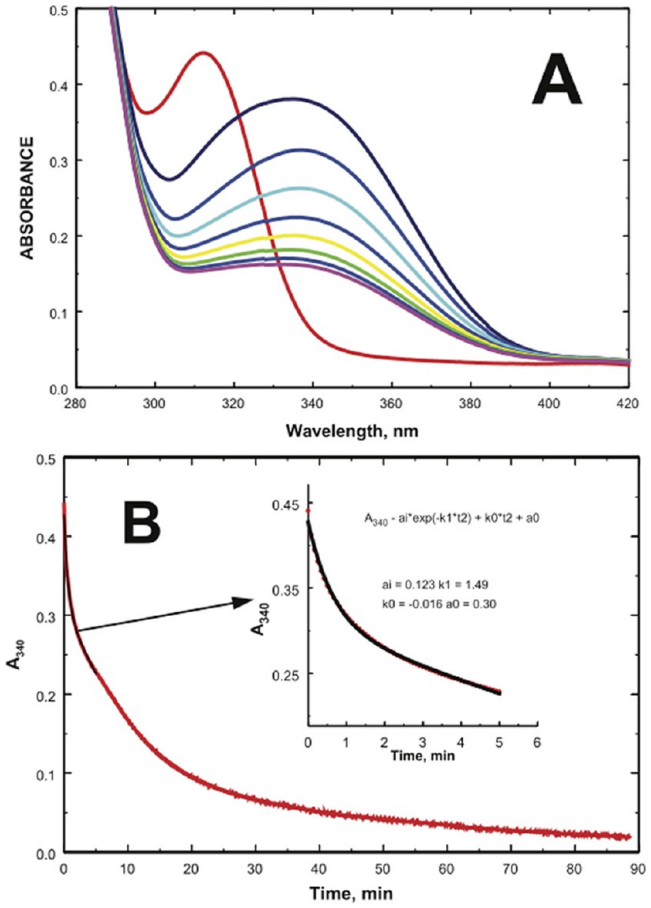

Figure 6. DithioHMG-CoA is a slow substrate. (A) Plots of absorbance vs wavelength at different times during the reaction of dithio-HMG-CoA and NADH in the presence of HMGR. The scan with a maximum near 312 nm (red line) is the spectrum of the HMGR–dithio-HMG-CoA complex before the reaction was initiated. The reaction was started by adding NADH to this mixture and restarting the spectrophotometer immediately at a scan rate of 60 nm/min from 450 to 240 nm. Scans were collected manually at 4 min intervals with the exception of the last scan, which was at an 8 min interval. The reaction mixture contained 20 μM *S. aureus* HMGR, 30 μM dithio-HMG-CoA, 80 μM NADH, and 50 mM HEPES (pH 7.0). The decrease in the NADH absorbance at 340 nm can be clearly followed (first scan, black line; final scan, purple line). (B) Plot of absorbance at 340 nm vs time for the reaction of dithio-HMG-CoA and NADH in the presence of *S. aureus* HMGR. In this study, the reaction was started by adding enzyme to the reaction mixture. The other conditions were the same as those described for Figure 6A, except that the reaction was blanked with a completed reaction mixture. The reaction is clearly triphasic. The initial burst phase and part of the intermediate zero-order phase were fit by nonlinear least squares to the equation, which contains both exponential and linear terms, shown in the inset. The half-life of the burst phase is ~0.5 min, and the magnitude of the burst corresponds to the oxidation of one enzyme equivalent of NADH.

NADH. *P. mevalonii* HMGR was also used to catalyze the reduction of dithio-HMG-CoA by NADH. The conditions for this study were the same as those described in the legend of Figure 6A except that only 10 μM instead of 20 μM enzyme was used. The reaction is again triphasic, though with this enzyme the initial burst phase is mostly within the dead time of the instrument. Taken together, these results demonstrate that dithio-HMG-CoA is a substrate for HMGR. The burst phase seems to correspond to approximately one enzyme equivalent of NADH oxidized and dithio compound reduced to the dithiohemiacetal or corresponding thiomevaldehyde. Because thiomevaldehyde should be easily reduced to the corresponding thioalcohol, we believe that the dithiohemiacetal is the most stable intermediate in the reaction coordinate and that decomposition of the C–S bond is rate-determining.

Dithio-HMG-CoA–NADH Structure. Given the finding that dithio-HMG-CoA is a substrate for HMGR, with a rapid first reduction reaction and a rate-limiting step further along the reaction path, we conducted an experiment hoping to trap the intermediate for this first hydride transfer. The experiment involved soaking an HMG-CoA reductase crystal in a 3.3 mM solution of dithio-HMG-CoA. This complex was then exposed to a solution containing 1.5 mM NADH with the goal of reacting sufficient substrate to produce the hemiacetal intermediate in the crystal, but not so much as to exchange nucleotide and go on to products.

The resulting reductase–dithio-HMG-CoA–NADH structure was strikingly different from the structure with HMG-CoA alone. The bonds around the C1 atom were no longer in one plane but rather took on a pyramidal configuration with each bond separated by 109° from the next (Figure 4C). This geometry is consistent with the transfer of a hydride from the NADH to the thioester, reducing the sp^2 orbital of the C1 atom to a hemiacetal sp^3 orbital. In addition, compared to the binary HMG-CoA–enzyme structures (RPMS and and RPM3SS), the carbonyl bond is rotated 120° toward the nicotinamide ring of NAD^+. This positions the carbonyl oxygen (sulfur in the slow substrate) within hydrogen bonding distance of catalytic residues Glu83 (3.0 Å) and Lys267 (3.4 Å) and 3.2 Å from the C4 hydride donor atom of the nicotinamide ring (Figures 4C and 8). This combination of movements places the hemiacetal in an ideal location for the second hydride transfer (once the nucleotide is exchanged) and the creation of free CoA and mevalonate.

These changes in geometry and orientation of the thioester are propagated though the pantothenic acid portion of the dithio-HMG-CoA causing the first amide bond (Figure 1), the one closest to the thioester/hemiactal, to rotate 180° (Figure 7). This positions the amide nitrogen to make a hydrogen bond both to the hydroxyl of Ser85 on the large domain (2.6 Å) and to His381 on the first helix of the flap domain [2.7 Å (Figure 8)]. While Ser85 has not previously been recognized as a catalytically important residue, an amino acid alignment shows that it is conserved across the prokaryotic homologues of HMGR.

In addition to the reduction of the dithio-HMG-CoA, electron density for the NAD^+ was also seen in the active site (Figure 4C). The nicotinamide ring appears at the dimer interface immediately adjacent to the HMG-CoA hemiacetal. The nucleotide appears to have a flat ring conformation and a 27° rotation of the carboxyamide group relative to the nicotinamide ring, suggesting transfer of the hydride to the dithio-HMG-CoA thioester.[30] In contrast to the HMG-CoA ligand, NAD^+ has many interactions directly with the enzyme, with all portions of the ligand participating in nucleotide–protein hydrogen bonds.

Closing of the Flap Domain. In addition to the binding of ligands and conversion of HMG-CoA to the reaction intermediate, difference ($F_o - F_c$) electron density consistent with the ordering of the 50 C-terminal residues of the flap domain was found. It was found to be composed of three

dx.doi.org/10.1021/bi400335g | *Biochemistry* 2013, 52, 5195–5205

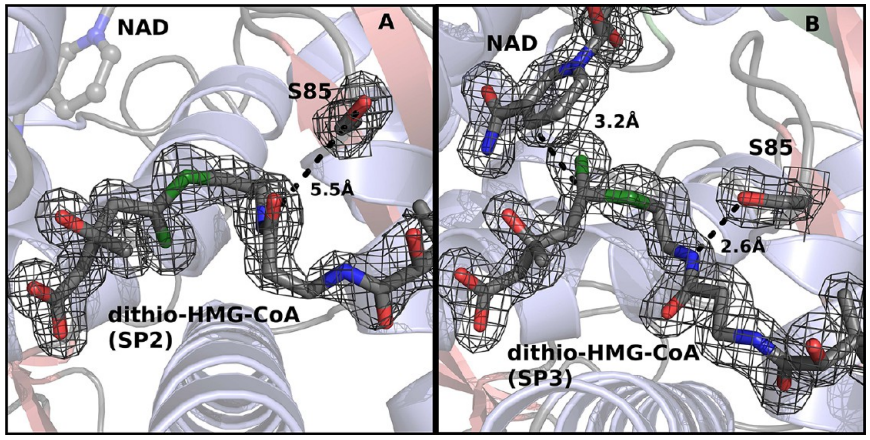

Figure 7. Adaptation of serine 85 to the formation of the hemiacetal. (A) Configuration of dithio-HMG-CoA and the protein loop containing serine 85 in the single-substrate complex (RPMS). The nucleotide is not present in this structure but is imported from the ternary complex structure (RPMU) for the purpose of reference. The hydroxyl of the serine is oriented away from the ligand, and the first amide bond of the HMG-CoA is turned away and distant from the serine. The electron density shown is the final refined $2F_o - F_c$ density contoured at 1.2σ. The Real Space correlation coefficient for the dithio-HMG-CoA is 0.884.[35] (B) These same structures, but after the formation of the hemiacetal (RPMU). Note the thioester of the dithio-HMG-CoA has taken on the tetrahedral configuration of the hemiacetal and has been reoriented close to the nicotinamide ring. The first pantothenic amide bond has rotated such that its nitrogen can make a 2.6 Å hydrogen bond to the hydroxyl of the rotated Ser85. The electron density shown is again the refined $2F_o - F_c$ density contoured at 1.2σ. The Real Space correlation coefficient for the NAD ligand is 0.939 and that of the dithio-HMG-CoA 0.926.[35] The red and green ribbons show the β-strands of monomers A and B, respectively. This figure was prepared using Pymol.[34]

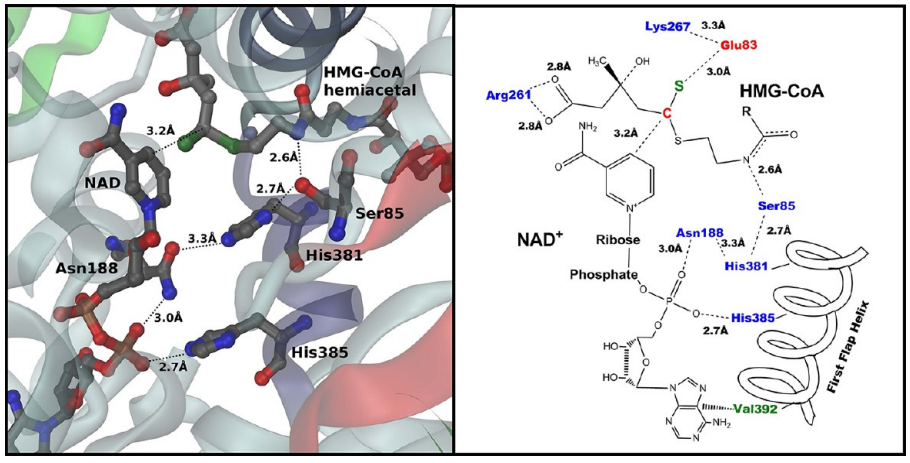

Figure 8. Hydrogen bonding network formed with creation of the hemiacetal intermediate. The ligands modeled here are from the structure (RPMU) in which the NADH has reduced the dithio-HMG-CoA to its hemiacetal form. Serine 85 has rotated to interact with the first amide bond of CoA and His381. The hydrogen bonding network continues with connections through Asn188, and from there through the NAD phosphate to His385. The first helix of the flap domain, which contains His381 and His385, is colored light blue extending down the center of the figure. Red and green β-strands are from monomers A and B, respectively. This figure was prepared using Pymol.[34]

helices (residues 377−394, 399−410, and 416−426) that cover the active site (Figure 3C) and positions residue His381 that provides the hydrogen for the CoA leaving group.[31] Significant hydrogen bonds between the residues in the flap subdomain and the enzyme or ligands include the already mentioned 2.7 Å interaction between Ser85 and His381 (Figure 8). This histidine side chain also has a potential hydrogen bond to the side chain oxygen of Asn188 (3.3 Å). One turn further along this helix is His385 that makes a hydrogen bond to the phosphoryl oxygen of the adenine phosphorus of NAD^+ (2.7 Å). The next interaction between this flap helix and the main body of the enzyme is with Val392, which helps to create the hydrophobic pocket around the adenine of NAD^+. Remaining contacts with the flap domain are distant from the active site and involve only the third flap helix, which lies against the small domain.

Interactions among HMG-CoA, NAD^+, and the Flap Domain. As the hydrogen bonding of the different ligands to the enzyme has been discussed in isolation, it may not be clear that the development of the hemiacetal, the binding of NAD(H), and the closing of the flap domain come together to create a hydrogen bond system uniting the three (Figure 8). One terminus of this system is the amide nitrogen of the hemiacetal HMG-CoA. As discussed above, the transformation of the geometry of the C1 atom from flat to pyramidal upon reduction from the thioester to the hemiacetal rotates the first amide so that the nitrogen interacts with the hydroxyl of Ser85 in the large domain (2.6 Å). This same oxygen hydrogen bonds to His381 (2.7 Å) located on the first helix of the flap domain,

dx.doi.org/10.1021/bi400335g | *Biochemistry* 2013, 52, 5195−5205

Table 2. Kinetic Parameters of the Wild-Type (WT) and S85A Mutant Enzymes[a]

			K_m (mM)		
enzyme	V_{max}[b]	% V_{max}	mevalonate	CoA	NAD^+
WT	38 ± 8	100	0.12 ± 0.02	0.090 ± 0.02	0.24 ± 0.00
S85A	1.3 ± 0.3	3	0.19 ± 0.05	0.48 ± 0.07	1.56 ± 0.49

[a]Experimental data are for duplicate or triplicate assays. [b]V_{max} is expressed as specific activity (micromoles of NADH produced per minute per milligram of protein).

stabilizing the subdomain and positioning this catalytic residue in the active site. The other nitrogen in the imidazole ring of His381 interacts with the side chain oxygen of Asn188 in the small domain (3.3 Å), which at the same time has a hydrogen bond between its side chain nitrogen and a phosphoryl oxygen of NAD^+ (3.0 Å). Another oxygen, associated with the same phosphorus, continues the thread by forming a hydrogen bond to His385 (2.7 Å), again on the same first helix of the flap domain as His381. From this point, the bonding pattern merges into the secondary structural elements of the flap domain. Thus, this string of hydrogen bonds knits together the two ligands and the flap domain and positions His381 for its catalytic role, protonating the CoA leaving group.

S85A Mutation. Serine 85 has not previously been identified as a catalytically important residue in prokaryotic HMG-CoA reductases. To further investigate this observation, a mutation was made, changing this residue to an alanine. Expression and purification of this mutant enzyme were accomplished using the same procedures that were used for the wild-type enzyme (see Experimental Procedures). Activity assays showed this mutant has a V_{max} of 1.3 μmol of NAD^+ reduced min^{-1} (mg of protein)$^{-1}$, 30-fold lower than that of the wild-type enzyme (Table 2). Relative to the wild-type enzyme, mutant enzyme S85A has the same K_m for mevalonate and similar but slightly higher (5−6-fold) K_m values for CoA and NAD^+ (Table 2).

GLIDE Calculation of Relative Binding Energies. The molecular docking program GLIDE (Schrödinger, LLC) was used to calculate the binding between the various forms of the ligand and the protein. This was calculated against the rigid crystallographic structures of the ligands against the protein. No refinement of the ligand was done. The calculated energy is reported as a unitless "score" value by the program, with the more negative numbers representing stronger binding. The score for the HMG-CoA−enzyme structure (RPMS) was calculated to be −9.9, that for the NAD^+−HMG-CoA structure (PDB entry 1QAX) to be −8.8, and that for the hemiacetal−enzyme model (RPMS) to be −12.8.

DISCUSSION

Between the enzyme structure with HMG-CoA bound and the one with both NAD^+ and the hemiacetal, there is a wide gulf of structural information missing. However, the literature offers a reasonable model for the trajectory between these two end points. The nonproductive enzyme complex, HMG-CoA−NAD^+ (PDB entry 1QAX), while not an intermediate in the reaction sequence, does have some characteristics to recommend it as a model for a transition structure. In particular, both the nucleotide and HMG-CoA ligand are bound, and the C-terminal flap is ordered and positioned over the site of hydride transfer. In addition, the carbonyl carbon of the thioester bond, while still demonstrating a flat, unreduced geometry, is now pointed toward the catalytic Glu83 and Lys267 residues and is much closer to the C4 hydride donor position of the nicotinamide ring than in the HMG-CoA alone structure (Figure 4B). With this role as an ersatz intermediate model in mind, it is interesting to note the evolution of the characteristics of the hemiacetal−enzyme complex as they develop through the three structures.

Evolution of Catalysis. Taking these three models (HMG-CoA alone, NAD^+−HMG-CoA complex, and NAD^+−hemiacetal complex), we can follow the changes in the enzyme and ligands as the reaction proceeds (Figure 1 for schematic and Figure 4 for structure). HMG-CoA binds with the thioester carbonyl pointed away from the active site (Figure 4A), the flap disordered, and no interaction between CoA and Ser85 (Figure 7A). NADH then binds with an accompanying ∼120° rotation of the thioester carbonyl toward the active site side chains (Figure 4B). As a consequence of this rotation, the HMG portion of the ligand is pulled up and out of its pocket, disrupting one of the hydrogen bonds between Arg261 and the HMG carboxyl group (Figure 5). In addition, the flap becomes ordered, though the Ser85−His381 hydrogen bonding network is not yet formed. As the hydride is transferred from the NADH to HMG-CoA, the thioester is reduced from the flat geometry consistent with an sp^2 molecular orbital to a pyramidal geometry consistent with an sp^3 orbital hemiacetal (Figure 4C). This change allows the ligand atoms to settle back into the binding pocket, restoring the hydrogen bonds with Arg261 [both again 2.8 Å (Figure 5)], and allows the hydrogen bond between the chiral alcohol of HMG-CoA and the amide of the nicotinamide ring to form. This reduction of the thioester and associated changes in geometry of the carbonyl carbon cause the 180° rotation of the first amide bond of CoA into a position where it hydrogen bonds to Ser85 and His 381. This seeds a network of hydrogen bonds that extends across both domains of the protein via Asn188 to interact with the NAD^+ phosphates and then back to bond with His385 in the first helix of the flap domain (Figure 8).

This interpretation of the evolution of these structures is supported by the energy profile of the reaction. This discussion lists the hydrogen bonds formed and broken as the HMG-CoA is transformed into the hemiacetal intermediate. This very qualitative approach suggests that the HMG-CoA alone has relatively few hydrogen bonds to the protein, that the 1QAX abortive complex creates more but loosens others, and finally that the hemiacetal is the most stable structure of all three. To put this on a more quantitative scale, we used the molecular docking program GLIDE (Schrödinger, LLC) to calculate the binding between the various forms of the ligand and the protein reported as a unitless score value by the program, with the more negative numbers representing stronger binding. The score of the HMG-CoA−enzyme structure (RPMS) was calculated to be −9.9, that of the NAD^+−HMG-CoA structure (PDB entry 1QAX) to be −8.8, and that of the hemiacetal−enzyme model (RPMS) to be −12.8. Thus, we have a classic energy curve of substrate binding evolving into a higher-energy (lower-binding energy) intermediate before going on to the

dx.doi.org/10.1021/bi400335g | Biochemistry 2013, 52, 5195−5205

more stable "product" of the hemiacetal. This additional stabilization of the bound hemiacetal intermediate compared to other configurations along the reaction pathway may well be the reason that previous investigators have failed to identify reaction intermediates of the enzyme in solution.

Supporting evidence also comes from the mutation of serine 85 to an alanine. Although this residue was not previously identified as being important to catalysis, the observations made possible by the structures presented here suggest that it plays a critical role in the reaction sequence. This role is supported by the kinetics of the S85A mutant enzyme that show it to be only 1/30th as active as the native form, while having K_m values very similar to that of the native form (Table 2).

In addition to the protein movements associated with these intermediate steps in catalysis, the crystallographic structures also provide further insight into the role of the catalytic residues. Previous functional analysis was based on the nonproductive complex of HMG-CoA and NAD^+ in the 1QAX structure.[9] This structure shows the ligand pulled up and out of the binding pocket relative to the position of the hemiacetal in the RPMU structure. This leads to the carbonyl oxygen being relatively closer to the lysine than the glutamate, so the lysine was reasonably proposed to function as the proton donor postreduction. Our structural analysis of the reaction coordinate suggests that 1QAX is a relatively high-energy intermediate state and that the hemiacetal position where the carbonyl oxygen is close to the glutamate is more stable and suggests Glu83 as an alternative proton donor for the reduction reaction. This alternative is reinforced by the recently published molecular modeling of the HMGR hydride transfer mechanism[32] that shows Glu83 to be the most likely general acid/base rather than Lys267. Lys267 then can function as part of an oxyanion hole that helps to stabilize the developing negative charge on the oxygen of the reaction intermediates.

In summary, we envision the HMG-CoA binding first with the thioester oriented away from the active site residues. As the NADH binds, the thioester is rotated up toward the relatively high energy state illustrated by the nonproductive NAD^+–HMG-CoA complex. As this state is approached, it becomes more and more advantageous for the hydride to be transferred. When the activation energy threshold and geometry are reached, the hydride is transferred, allowing the relaxation of the thioester into a hemiacetal pyramidal structure and donation of the proton from Glu83 to the oxyanion. This change in geometry drives the rotation of the first CoA amide bond and thereby the formation of the Ser85 web of hydrogen bonds. This interpretation of events, while consistent with the presented structures, mutational data, and supporting energy calculation, is qualified. One of the current projects in the laboratory is a time-resolved Laue experiment that will allow us to follow this catalytic evolution in real time, replacing our analysis based on static structures with real-time experimental data.

The structures and analysis presented here have allowed unprecedented insight into the molecular mechanism of catalysis. We have shown how the interplay of ligand binding and the fundamental geometric change of the thioester bond reduction drive changes in the ligand–protein interactions and energetics that tend to drive the reaction forward. In addition, it is seen that CoA, far from being a passive carrier of the substrate, performs a fundamental and unique role in the structural dynamics of catalysis.

■ ASSOCIATED CONTENT

Accession Codes

The coordinates associated with this publication have been deposited and validated by the Protein Data Bank. PDB accession codes for HMG-CoA reductase complexes: 4I6A for RPM3SS (complex with HMG-CoA without glycerol), 4I64 for RPMQS (high-resolution apoenzyme), 4I56 for RPMS (complex with dithio-HMG-CoA), and 4I4B for RPMU [complex with hemiacetal dithio-HMG-CoA and NAD(H)].

■ AUTHOR INFORMATION

Corresponding Author

*Department of Biology, Purdue University, Hockmeyer Hall of Structural Biology, 240 S. Martin Jischke Dr., West Lafayette, IN 47907. E-mail: cstauffa@purdue.edu. Telephone: (765) 494-4937. Fax: (765) 496-1189.

Funding

This work was directly supported by National Science Foundation Grant MCB-0444247 to C.V.S. and National Institutes of Health GM Traineeship T32 GM008296 to C.J.C. Use of the Advanced Photon Source was supported by the U.S. Department of Energy, Basic Energy Sciences, Office of Science, under Contract DE-AC02-06CH11357. Use of BioCARS Sector 14 was supported by the National Institutes of Health, National Center for Research Resources, via Grant RR007707. Use of IMCA-CAT beamline 17-ID (or 17-BM) at the Advanced Photon Source was supported by the companies of the Industrial Macromolecular Crystallography Association through a contract with Hauptman-Woodward Medical Research Institute.

Notes

The authors declare no competing financial interests.

■ ACKNOWLEDGMENTS

We thank the members of the Markey Center for Structural Biology and the Purdue Center for Cancer Research for support of this research.

■ REFERENCES

(1) Goldstein, J. L., and Brown, M. S. (1990) Regulation of the mevalonate pathway. *Nature 343*, 425–430.

(2) Johnson, E. A., and Schroeder, W. A. (1996) Microbial carotenoids. *Adv. Biochem. Eng. Biotechnol. 53*, 119–178.

(3) Reusch, V. M., Jr. (1984) Lipopolymers, isoprenoids, and the assembly of the Gram-positive cell wall. *Crit. Rev. Microbiol. 11*, 129–155.

(4) Bochar, D. A., Stauffacher, C. V., and Rodwell, V. W. (1999) Sequence comparisons reveal two classes of 3-hydroxy-3-methylglutaryl coenzyme A reductase. *Mol. Genet. Metab. 66*, 122–127.

(5) Istvan, E. S. (2001) Bacterial and mammalian HMG-CoA reductases: Related enzymes with distinct architectures. *Curr. Opin. Struct. Biol. 11*, 746–751.

(6) Wilding, E. I., et al. (2000) Identification, evolution, and essentiality of the mevalonate pathway for isopentenyl diphosphate biosynthesis in Gram-positive cocci. *J. Bacteriol. 182*, 4319–4327.

(7) Qureshi, N., et al. (1976) Kinetic analysis of the individual reductive steps catalyzed by β-hydroxy-β-methylglutaryl-coenzyme A reductase obtained from yeast. *Biochemistry 15*, 4191–4198.

(8) Lawrence, C. M., Rodwell, V. W., and Stauffacher, C. V. (1995) Crystal structure of *Pseudomonas mevalonii* HMG-CoA reductase at 3.0 angstrom resolution. *Science 268*, 1758–1762.

(9) Tabernero, L., et al. (1999) Substrate-induced closure of the flap domain in the ternary complex structures provides insights into the

mechanism of catalysis by 3-hydroxy-3-methylglutaryl-CoA reductase. *Proc. Natl. Acad. Sci. U.S.A. 96*, 7167−7171.
(10) Schulz, G. E. (1992) Binding of nucleotides by proteins. *Curr. Opin. Struct. Biol. 2*, 61−67.
(11) Frimpong, K., and Rodwell, V. W. (1994) Catalysis by Syrian hamster 3-hydroxy-3-methylglutaryl-coenzyme A reductase. Proposed roles of histidine 865, glutamate 558, and aspartate 766. *J. Biol. Chem. 269*, 11478−11483.
(12) Beach, M. J., and Rodwell, V. W. (1989) Cloning, sequencing, and overexpression of mvaA, which encodes *Pseudomonas mevalonii* 3-hydroxy-3-methylglutaryl coenzyme A reductase. *J. Bacteriol. 171*, 2994−3001.
(13) Lawrence, C. M., et al. (1995) Crystallization of HMG-CoA reductase from *Pseudomonas mevalonii*. *Acta Crystallogr. D51*, 386−389.
(14) Otwinowski, Z., and Minor, W. (1997) Processing of X-ray Diffraction Data Collected in Oscillation Mode. In *Macromolecular Crystallography* (Carter, C. W., and Sweet, R. M., Eds.) pp 307−326, Academic Press, New York.
(15) Brunger, A. T., et al. (1998) Crystallography & NMR system: A new software suite for macromolecular structure determination. *Acta Crystallogr. D54* (Part 5), 905−921.
(16) Kleywegt, G. J., Henrick, K., Dodson, E. J., and van Aalten, D. M. (2003) Pound-wise but penny-foolish: How well do micromolecules fare in macromolecular refinement? *Structure 11*, 1051−1059.
(17) Allen, F. H. (2002) The Cambridge Structural Database: A quarter of a million crystal structures and rising. *Acta Crystallogr. B58*, 380−388.
(18) Jones, T. A., Zou, J. Y., and Kjeldgaard, M. (1991) Improved methods for building protein models in electron-density and location of errors in these models. *Acta Crystallogr. A47*, 110−119.
(19) Kleywegt, G., and Jones, A. (1997) Model Building and Refinement Practice. In *Macromolecular Crystallography* (Carter, C. W., and Sweet, R. M., Eds.) pp 208−229, Academic Press, New York.
(20) Murshudov, G. N., Vagin, A. A., and Dodson, E. J. (1997) Refinement of macromolecular structures by the maximum-likelihood method. *Acta Crystallogr. D53*, 240−255.
(21) Winn, M. D., Isupov, M. N., and Murshudov, G. N. (2001) Use of TLS parameters to model anisotropic displacements in macromolecular refinement. *Acta Crystallogr. D57*, 122−133.
(22) Brunger, A. T. (1992) Free R value: A novel statistical quantity for assessing the accuracy of crystal structures. *Nature 355*, 472−475.
(23) Kleywegt, G., and Jones, A. (1995) Where freedom is given, liberties are taken. *Structure*, 535−540.
(24) Chen, V. B., et al. (2010) MolProbity: All-atom structure validation for macromolecular crystallography. *Acta Crystallogr. D66*, 12−21.
(25) Laskowski, R. A., et al. (1993) Procheck: A program to check the stereochemical quality of protein structures. *J. Appl. Crystallogr. 26*, 283−291.
(26) Markley, J. L., et al. (1998) Recommendations for the presentation of NMR structures of proteins and nucleic acids: IUPAC-IUBMB-IUPAB inter-union task group on the standardization of data bases of protein and nucleic acid structures determined by NMR spectroscopy. *Eur. J. Biochem. 256*, 1−15.
(27) Wang, Y., Darnay, B. G., and Rodwell, V. W. (1990) Identification of the principal catalytically important acidic residue of 3-hydroxy-3-methylglutaryl coenzyme A reductase. *J. Biol. Chem. 265*, 21634−21641.
(28) Wrensford, L. V., Rodwell, V. W., and Anderson, V. E. (1991) 3-Hydroxy-3-methylglutaryldithio-coenzyme A: A potent inhibitor of *Pseudomonas mevalonii* HMG-CoA reductase. *Biochem. Med. Metab. Biol. 45*, 204−208.
(29) Sikkema, K. D., and O'Leary, M. H. (1988) Synthesis and study of phosphoenolthiopyruvate. *Biochemistry 27*, 1342−1347.
(30) Wu, Y. D., and Houk, K. N. (1991) Theoretical evaluation of conformational preferences of NAD^+ and NADH: An approach to understanding the stereospecificity of NAD^+/NADH-dependent dehydrogenases. *J. Am. Chem. Soc. 113*, 2353−2358.
(31) Darnay, B., Wang, Y., and Rodwell, V. (1992) Identification of the catalytically important histidine of 3-hydroxy-3- methylglutaryl-coenzyme A reductase. *J. Biol. Chem. 267*, 15064−15070.
(32) Haines, B. E., Steussy, C. N., Stauffacher, C. V., and Wiest, O. (2012) Molecular modeling of the reaction pathway and hydride transfer reactions of HMG-CoA reductase. *Biochemistry 51*, 7983−7995.
(33) *ChemDraw ultra 12.0* (2010) Cambridgesoft.
(34) Schrodinger, L. *The PyMOL molecular graphics system*, version 1.3, Schrödinger, LLC, New York.
(35) Adams, P. D., et al. (2010) PHENIX: A comprehensive python-based system for macromolecular structure solution. *Acta Crystallogr. D66*, 213−221.